Sputtering of beryllium oxide by deuterium at various temperatures simulated with molecular dynamics

Etienne A Hodille, Jesper Byggmästar, E Safi, Kai Nordlund

▶ **To cite this version:**

Etienne A Hodille, Jesper Byggmästar, E Safi, Kai Nordlund. Sputtering of beryllium oxide by deuterium at various temperatures simulated with molecular dynamics. Physica Scripta, 2020, T171, pp.014024. ⟨10.1088/1402-4896/ab43fa⟩. ⟨hal-02901332⟩

HAL Id: hal-02901332

https://hal.science/hal-02901332v1

Submitted on 17 Jul 2020

HAL is a multi-disciplinary open access archive for the deposit and dissemination of scientific research documents, whether they are published or not. The documents may come from teaching and research institutions in France or abroad, or from public or private research centers.

L'archive ouverte pluridisciplinaire **HAL**, est destinée au dépôt et à la diffusion de documents scientifiques de niveau recherche, publiés ou non, émanant des établissements d'enseignement et de recherche français ou étrangers, des laboratoires publics ou privés.

HAL Authorization

ResearchGate

See discussions, stats, and author profiles for this publication at: https://www.researchgate.net/publication/339638946

Sputtering of beryllium oxide by deuterium at various temperatures simulated with molecular dynamics

Article *in* Physica Scripta · January 2020

DOI: 10.1088/1402-4896/ab43fa

CITATIONS
0

READS
50

4 authors, including:

E.A. Hodille
Atomic Energy and Alternative Energies Commission
37 PUBLICATIONS **390** CITATIONS
SEE PROFILE

Jesper Byggmästar
University of Helsinki
23 PUBLICATIONS **94** CITATIONS
SEE PROFILE

Kai Nordlund
University of Helsinki
647 PUBLICATIONS **17,434** CITATIONS
SEE PROFILE

Some of the authors of this publication are also working on these related projects:

Multi-scale model for hydrogen transport and recycling from Porous Graphite View project

Extreme Irradiation of Materials: Fusion Reactor Conditions in ITER and Beyond (EXMAT) View project

All content following this page was uploaded by E.A. Hodille on 03 March 2020.

The user has requested enhancement of the downloaded file.

Preprint of article accepted for publication in Physica Scripta

Sputtering of beryllium oxide by deuterium at different temperatures simulated with molecular dynamics

E A Hodille, J Byggmästar, E Safi, K Nordlund

Department of Physics, University of Helsinki, P. O. Box 43, FI-00014,Finland

E-mail: etienne.hodille@helsinki.fi

Abstract. The sputtering yield of beryllium oxide (BeO) by incident deuterium (D) ions, for energies from 10 eV to 200 eV, has been calculated for temperatures between 300 K and 800 K using classical molecular dynamics. First, cumulative irradiations are done to build up a concentration of D in the material, equal to the one experimentally measured, that varies from 0.12 atomic fraction (300 K - 500 K) to 0.02 atomic fraction (800 K). After building up the concentration of D, non-cumulative irradiations are done to estimate the sputtering yields of BeO. For all incident energies, the sputtering yield peaks at 500 K, being closely related to the decrease of the concentration of D above this temperature. While for 10 eV, the concentration of D on the surface drives the temperature dependence, above 30 eV, it is the amount of surface damage created during the cumulative irradiation.

Keywords: Plasma-wall interactions, Molecular dynamics, Beryllium oxide, Deuterium

1. Introduction

Beryllium (Be) is the chosen material for the first wall of JET [1, 2] and ITER [3]. Ions coming from the plasma can lead to sputtering of this material, reducing the life time of the plasma-facing components and creating a source of impurity for the plasma. In addition, the sputtered material can migrate in the edge plasma and be redeposited on surfaces creating a deposited layer that is expected to be the main media for fuel retention in ITER [4, 5]. It is thus important to estimate the sputtering of Be materials in a fusion environment.

Be oxidises easily, and a thin Beryllium oxide (BeO) layer can be formed with a small pressure of oxygen. Thus, BeO layers can be formed between plasmas and quickly removed in strong sputtering area during plasma operation (in limiter plasma for instance). BeO can also be formed during off-normal events like melting of Be, as BeO inclusions have been observed by Raman spectroscopy in melted regions [6, 7]. The sputtering of BeO by deuterium (D) ions is thus of importance for the description and understanding of the plasma-wall interactions.

In this work, we use molecular dynamics (MD) to estimate the sputtering yields of BeO by D ions. In a previous study, MD has been used to determine these sputtering yields at 300 K [8]. During tokamak operations, the temperature of the first wall can rise above 300 K. Here, the MD simulations have been extended to provide estimations of sputtering yields of BeO up to 800 K.

2. Method

The irradiation of BeO was simulated with classical MD using the MD code PARCAS [9]. The simulation cells contain three species: beryllium (Be), oxygen (O) and Deuterium (D). To describe the interactions between these species, Tersoff-like potentials [10, 11] have been used. For these interactions, D atoms are considered as H atoms with a mass of 2.014 atomic mass units. The Be-Be and Be-H potential are both taken from [12] (version II), the H-H potential is taken from [13], the O-O is taken from [14], the Be-O is taken from [15] and the O-H part is taken from [8]. The full Be-O-H potential was previously shown to give good agreement between simulated and experimental sputtering yields [8], and is therefore well-suited for plasma-wall interaction simulations.

In [8], it is shown that the sputtering yield increases with c_D in the material. The best comparison between MD and experimental sputtering yields is obtained at 300 K for $c_\mathrm{D} \approx 0.12$ atomic fraction (at.fr.) which is the saturation concentration of deuterium in BeO determined experimentally for irradiation at 300 K [16]. Thus, for the present simulations at different temperatures, the temperature dependent values of c_D in BeO are also used. Roth *et al* [17] as well as Alimov *et al* [18] reports those values of c_D for temperatures between 300 K and 773 K. They are shown on figure 1. Both experimental studies agree on the evolution of c_D in BeO with temperatures: c_D is about constant (equal to 0.12 at.fr.) from 300 K to 500 K and it drops above 500 K.

The simulation set-up used in this paper is the same as in [8]: a wurtzite BeO cell with a $(000\bar{1})$ surface is irradiated with ion energies of 10 eV, 30 eV, 50 eV, 80 eV, 140 eV and 200 eV. The irradiated temperatures are 400 K, 500 K, 600 K, 700 K and 800 K. The sputtering data at 300 K are taken from [8] and have

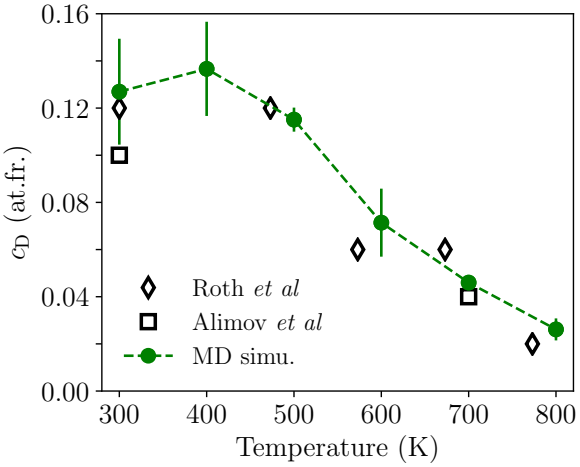

Figure 1: Evolution of the deuterium concentration, c_D, with temperatures. The open symbol are the experimental values reported by Roth *et al* [17] and Alimov *et al* [18] (experiments). The closed circles are the value of the deuterium concentration, c_D, used in the MD simulations (averaged on all 6 energies used in this paper). The error bars are the standard deviation over all 6 energies.

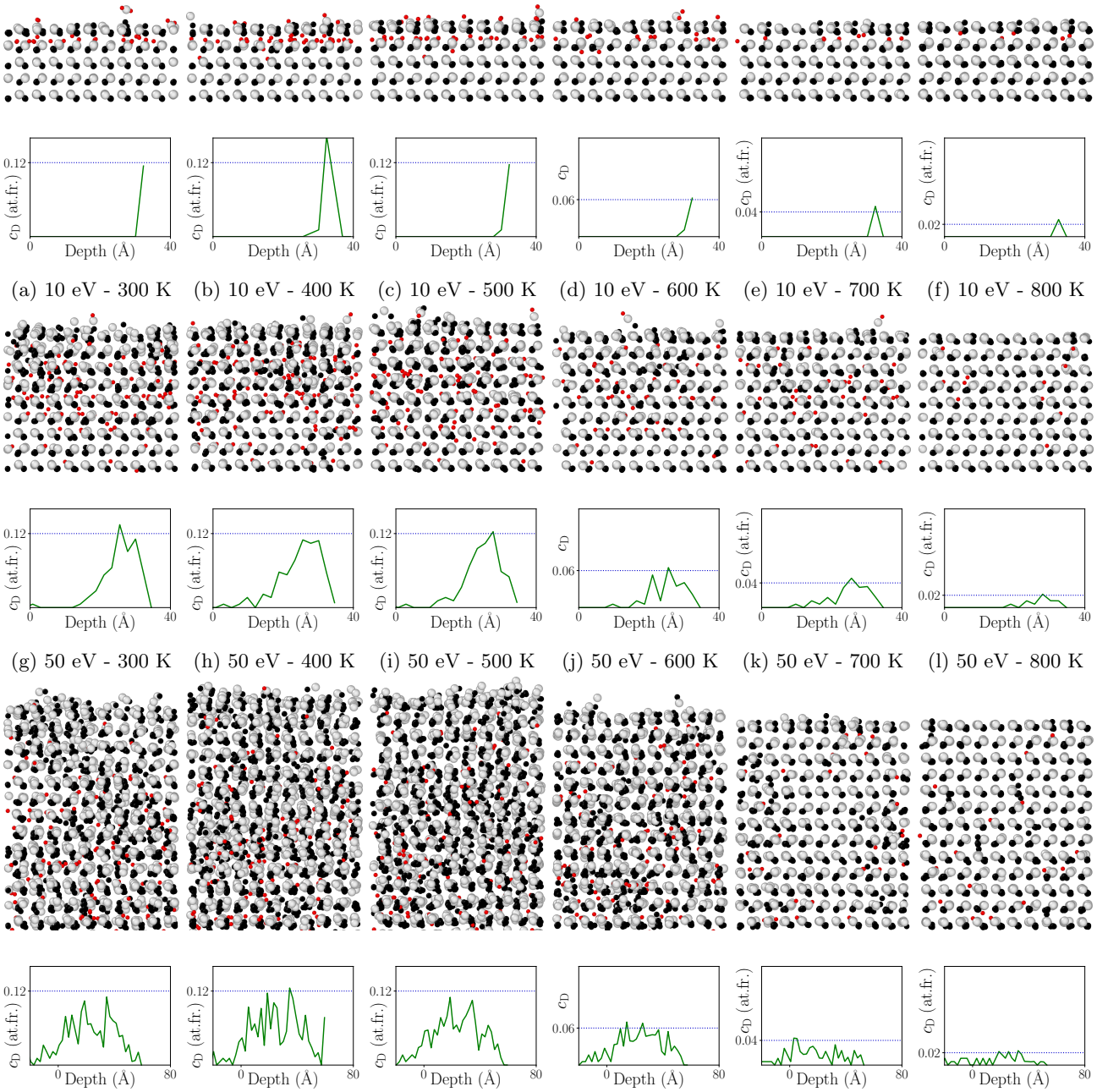

(a) 10 eV - 300 K (b) 10 eV - 400 K (c) 10 eV - 500 K (d) 10 eV - 600 K (e) 10 eV - 700 K (f) 10 eV - 800 K

(g) 50 eV - 300 K (h) 50 eV - 400 K (i) 50 eV - 500 K (j) 50 eV - 600 K (k) 50 eV - 700 K (l) 50 eV - 800 K

(m) 140 eV - 300 K (n) 140 eV - 400 K (o) 140 eV - 500 K (p) 140 eV - 600 K (q) 140 eV - 700 K (r) 140 eV - 800 K

Figure 2: Simulation cells obtained by the cumulative irradiation and used for the non-cumulative irradiations for the different temperatures from 300 K to 800 K and incident energies of 10 eV ((a) to (f)), 50 eV ((g) to (l)) and 140 eV ((m) to (r)). Top: Snapshot of the cells, obtained with the OVITO software [19], with O atoms in grey, Be in black and D in red. Bottom: Evolution of the deuterium concentration c_D in the depth for the considered cells. The experimental concentrations are shown with a dotted line.

been obtained with the exact same procedure. The cell is 25×24 Å^2 in the (x,y) plane and is elongated in the z direction (Z=68 Å for $E_{inc} < 80$ eV and Z=104 Å for ≥80 eV). Each irradiation lasts for 7000 fs and prior to any irradiation, the box is randomly shifted over the periodic boundaries in the x and y direction to simulate a uniform bombardment. More details on the simulation set-up (relaxation of the box, temperature control, incident angle) can be found in [8].

As in [8], first, cumulative irradiations are run to build up a D-rich layer. The cumulative irradiations are stopped when the D concentration in this layer is

comparable to the experimental ones. The values of c_D obtained during this first step are shown in figure 1 (averaged over the 6 energies). For the lowest temperatures, these concentrations are reached after about 100 (for 10 eV) or 400 (for 200 eV) impacts, while only few tens of impacts are needed for the highest temperatures (lowest c_D). The cells obtained this way and used in the non-cumulative irradiation are shown in figure 2 for incident energies of 10 eV, 50 eV and 140 eV for the different temperatures. For 30 eV (80 eV), the cells are similar to the ones obtained for 50 eV with more (less) D atoms on the surface. For 200 eV, the simulation cells are similar to the ones obtained for 140 eV with a more pronounced swelling of the cell for the highest value of c_D. The D depth profiles are limited to the implantation zone (few nm below the surface) as the diffusion coefficient of H in BeO is large [20, 21] meaning that no diffusion can be captured at the MD time scale.

After building up the relevant deuterium concentration in the material, 10000 non-cumulative impacts are simulated to determine the sputtering yields of BeO, Y_{BeO}, calculated as the average number of sputtered Be and O atoms over incoming D ions. The standard deviation over all individual bombardments are used to provide error bars to the estimated sputtering yields. Again, to simulate a uniform bombardment, the simulation cell is randomly shifted over the periodic boundaries in the x and y direction before any impacts.

3. Results and discussion

3.1. Evolution of Y_{BeO} with the temperature

The sputtering yields calculated by MD calculations for the different incident energies and temperatures are reported in figure 3 and are correlated to the evolution of c_D with temperature. Experimental data at room temperature on oxidized Be samples [22, 24] and sintered BeO [23] are also reported. For all energies, Y_{BeO} increases from 300 K to 500 K as c_D is constant, and as soon as c_D decreases, Y_{BeO} decreases as well. Such peaking of the sputtering yield with temperature has already been reported for carbon-based materials [25, 26, 27] and Si [25] and is understood to be evidence of chemical sputtering [27]. Concerning BeO, the evolution of the sputtering yields with temperature has not been studied experimentally so far. However, concerning metallic Be, Nishijima *et al* [28] observed experimentally a decrease of the sputtering yield of plasma-deposited Be layer from 320 K to 570 K that they attributed to a decrease of the deuterium retention at 570 K. In addition, the sputtering yield of Be in JET has also been shown to decrease from 200°C (473 K) to 400°C (673

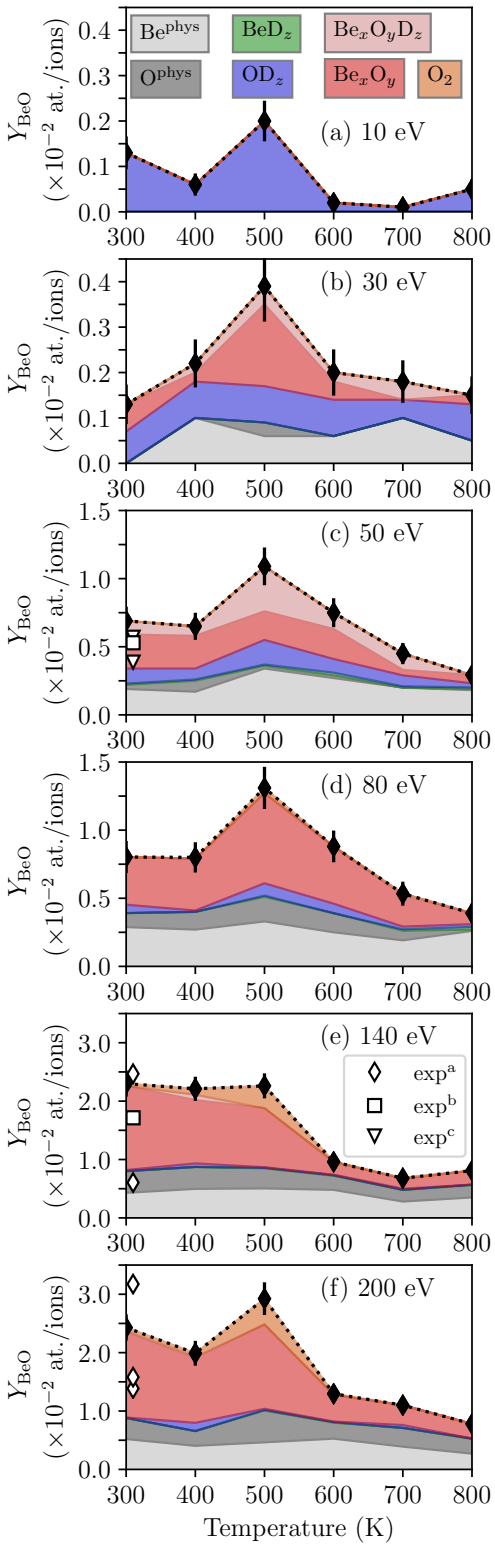

Figure 3: Evolution of the MD sputtering yield Y_{BeO} with the temperatures. The contributions of single Be atoms (Be^{phys}), single O atoms (O^{phys}), BeD$_z$, OD$_z$, Be$_x$O$_y$, Be$_x$O$_y$D$_z$ and O$_2$ are also shown. exp^a [22] (150 eV and 200 eV), exp^b [23] (50 eV and 150 eV) and exp^c [24] (50 eV and 60 eV)

K) [29, 30]. It is explained by the decrease of c_D in Be with temperature, diminishing the production of BeD molecules as shown in MD simulations [31]. Thus, to investigate further the observed peaking of Y_{BeO} at 500 K, we distinguished the different sputtering products as follows: single O/Be atoms, BeD_z and OD_z molecules, Be_xO_y, $Be_xO_yD_z$ and O_2 molecules. For OD_z molecules, z is equal to 1 or 2 (z=2 is heavy water molecules). The contribution of each of these products is shown in figure 3.

3.2. Physical sputtering of Be and O

The single atoms are produced through physical sputtering processes and no strong temperature evolution can be determined for physical sputtering of Be and O. One can still note that for 30 eV, there is no single Be sputtered at 300 K while there are at higher temperature. Regarding the obtained sputtering yields of $\approx 1 \times 10^{-3}$, this represents about 10 sputtering events among the 10000 non-cumulative irradiations. Thus, sputtering of few Be could have been missed by the limited number of impacts.

In figure 3, one can roughly estimate the threshold for physical sputtering of Be and O. It is between 10 and 30 eV for Be while it is around 30 eV for O. This difference makes sense considering the difference of mass between these two elements.

3.3. Swift chemical sputtering of OD_z molecules

The BeD_z and OD_z molecules are mostly produced by swift chemical sputtering (SCS) [8, 32]. The proportion of BeD_z is at maximum a few percent while the one of OD_z is 100% for 10 eV. The predominance of OD_z comes mostly from the fact that the OD dimer is much more stable than BeD [8].

For 10 eV, this contribution, which represents all the sputtering events, peaks at 500 K and then drops by one order of magnitude as c_D decreases. In [8], we showed that the SCS mechanism is active for 10 eV $< E_{inc} \leq$ 80 eV for a perfect $(000\bar{1})$ surface. However, the presence of adsorbed D leads to the formation of O-D bonds, which loosen the bond of the O atoms to the rest of the material [8]. Such a bound O atom can then be sputtered by 10 eV D ions. The amount of O-D bonds on the surface for the highest values of c_D (300 K - 500 K) is obviously higher (figure 2(a) to (c)) than for the lowest values of c_D (700 K - 800 K). For 700 K and 800 K, no O-D bonds are actually on the surface and all the D atoms are below the surface (figure 2 (e), (f)).

For $E_{inc} \geq 30$ eV, the temperature dependence of the formation of OD_z through SCS is not as obvious, except for a slight increase from 400 K to 500 K at 50 eV. Indeed, other sputtering processes start to appear (physical sputtering, formation of $Be_xO_yD_z$ molecules). Thus, SCS leading to OD_z molecules contribute only to a few tens of percent at 30 eV, a few percent at 50 eV and 80 eV and almost 0 above that as the upper limit for this process is about 80 eV [8].

3.4. Sputtering of $Be_xO_yD_z$ molecules

In the Be-O potentials used here, the energy of the BeO dimer had to be overestimated by 1 eV/atom in order to have accurate cohesive energies for the bulk phases [15]. This could favor the formation of $Be_xO_yD_z$ molecules in our MD simulations that appear mostly as BeO dimer and BeOD molecules. However, BeO, BeOD and BeO_2 molecules have been observed experimentally by mass spectrometry after the bombardment of Be samples by an $(Ar^+ + D_2^+)$ mixture [33]. Thus, their formation in our MD simulations is not an artifact of the potential.

For $E_{inc} \geq$30 eV, as can be seen in figure 3, the temperature dependence of Y_{BeO} is mostly due to the sputtering of $Be_xO_y(D_z)$ molecules (including O_2). For most of the events involving $Be_xO_y(D_z)$ formation, the incident ion is not bound to the sputtered molecules: the initial interaction leading to the sputtering has a physical nature. It is the description of the chemically assisted physical sputtering (CAPS) suggested by Brezinsek *et al* [34]. In our previous simulations of irradiations of BeO at 300 K, we determined 4 processes leading to the production of these molecules via CAPS. First, there are two types of BeO physical sputtering mechanisms (direct and delayed) called $Y^{phys}_{Be_xO_yD_z}$. During a direct physical sputtering event, the incident D ion physically sputters one Be/O atom which drags with it one of its O/Be neighbors forming a BeO dimer. During a delayed physical sputtering event, the incident D atom physically sputters one atom in its way in the material, is back-scattered and sputters another atom in its way back. If both sputtered atoms were neighbors, they might be sputtered together within a short space and time window allowing them to stay bound as a BeO dimer (this is a rare event due to the conditions required for it). Trajectories for both mechanisms can be found in [8]. Then, there are two other processes active only on damaged surfaces, i.e. surfaces containing roughness and loosely bound groups of atoms (figure 2). The first is the delayed SCS sputtering during which an atom is kicked away from its initial position. It can then move on the surface and possibly interact with other atoms via the SCS mechanism releasing a molecules. The second is the detachment induced sputtering: on the damaged surface, there are atoms or groups of atoms that are more loosely bound to the surface than any atoms on

a pristine surface. If the incident D ion kicks off the atoms that bond a group of these atoms to the rest of the material, they can be detached from the surface. Trajectories for both mechanisms can also be found in [8]. Both processes are regrouped in $Y^{\mathrm{dam}}_{\mathrm{Be}_x\mathrm{O}_y\mathrm{D}_z}$.

For $c_{\mathrm{D}} \approx 0$ at.fr., with a perfect $(000\bar{1})$ surface, among these two processes, only $Y^{\mathrm{phys}}_{\mathrm{Be}_x\mathrm{O}_y\mathrm{D}_z}$ is active and it represents about 30 percent of the total sputtering yield [8]. In figure 3, for 700 K and 800 K ($c_{\mathrm{D}} < 0.04$ at.fr.), the contribution of $\mathrm{Be}_x\mathrm{O}_y(\mathrm{D}_z)$ is also about 30 percent and the irradiated surfaces are almost perfect $(000\bar{1})$ (figure 2). Thus, at these temperatures, only $Y^{\mathrm{phys}}_{\mathrm{Be}_x\mathrm{O}_y\mathrm{D}_z}$ is active.

On the other hand, for the highest values of c_{D} (300 K to 600 K), as seen in figure 2, the material is more damaged (and eventually amorphized). This amorphization and surface damage are expected in insulator material [35]: the energy threshold for this amorphization can be very low (about 0.01 keV/target atom) for material that are more covalent than ionic [35], which is the case of BeO [36]. Thus, it activates $Y^{\mathrm{dam}}_{\mathrm{Be}_x\mathrm{O}_y\mathrm{D}_z}$ for the highest values of c_{D} for which $Y_{\mathrm{Be}_x\mathrm{O}_y\mathrm{D}_z}$ contribute between 30 and 60/70 percent to the total sputtering yield. As a larger amount of irradiation is needed to build up the relevant value of c_{D}, the surfaces for higher c_{D} are more damaged than for low c_{D}. Thus, the decrease of c_{D} above 500 K induces a reduced amount of surface damage, leading to a decrease of $Y^{\mathrm{dam}}_{\mathrm{Be}_x\mathrm{O}_y\mathrm{D}_z}$ and hence also Y_{BeO} from 500 K to 800 K.

Despite $c_{\mathrm{D}}(300\ \mathrm{K}) > c_{\mathrm{D}}(600\ \mathrm{K})$, for 30 eV$\leq E_{\mathrm{inc}} \leq 80$ eV, there is $Y_{\mathrm{BeO}}(600\ \mathrm{K}) > Y_{\mathrm{BeO}}(300\ \mathrm{K})$, a pronounced increase of Y_{BeO} from 300 K to 500 K and a smooth decrease above 500 K. It means a thermally activated process either (i) increases the amount of surface damage when building up c_{D} or (ii) facilitates the sputtering of atoms thanks to the thermal motion. Both can play a role in the temperature behavior of Y_{BeO} but one can expect that the enhancement of Y_{BeO} by a higher thermal motion would be similar for any incident energies. As the peaking is only observed for $E_{\mathrm{inc}} \leq 80$ eV, it is most likely that the peaking of Y_{BeO} is due to a increase of the surface damage with the temperature (for constant c_{D}). Indeed, the depth profiles in figure 2 show that the D atoms are deposited much closer to the surface for 50 eV: the damage are close to (and eventually on) the surface. At 140 eV, the D atoms are much deeper in the bulk: even though the damage induced by the irradiations increases from 300 K to 500 K they are moslty located in the bulk and do not affect that much the surface and the sputtering yield. Thus, for all energies, the disorder and damage induced by the ion irradiations increases with the temperature (from 300 K to 500 K), but they affect the sputtering yield in that range of temperature only if they are close to the surface. This difference in deposition also leads to higher surface D concentrations at low energy, especially for 30 eV and 50 eV, leading to a higher relative contribution of $\mathrm{Be}_x\mathrm{O}_y\mathrm{D}_z$ in the total sputtering yield.

Finally, one can note that O_2 is only formed in high fraction at 500 K for $E_{\mathrm{inc}} \geq 140$ eV (figure 3). For these energies, the morphology of the surface damage (figure 2 m-r) favor the delayed SCS sputtering. O_2 can then be formed if an O atom migrating on the surface recombines with another one. The surface damage for $E_{\mathrm{inc}} \geq 140$ eV can also lead to the formation of adsorbed O_2 molecules as two O atoms are close together (one of their common Be neighbor being sputtered away during the cumulative irradiation). These O_2 molecules can be outgassed by the local increase of temperature created by the incident D ion impact. As the surface disorders are the highest at 500 K and as outgassing is also favored by higher temperature, this explains the high fraction of O_2 production at 500 K.

4. Conclusions

MD simulations of the irradiation of $(000\bar{1})$ wurtzite BeO surface at energies from 10 eV to 200 eV and temperatures from 300 K to 800 K have been carried out to estimate the variation of the BeO sputtering yield Y_{BeO} with temperature. First, cumulative irradiations were done to build a concentration of deuterium, c_{D} in the material. From experimental results, the value of c_{D} depends on the irradiation temperature [17, 18]: it is 0.12 at.fr. from 300 K to 500 K and it drops up to 0.02 at.fr. at 800 K. In the simulations, for all energies, Y_{BeO} follows the trends of $c_{\mathrm{D}}(T)$ above 500 K: it decreases as the concentration of deuterium decreases. In the temperature range where c_{D} is constant equal to 0.12 at.fr. (300 K - 500 K), Y_{BeO} increases. For 10 eV, only OD_z molecules are sputtered and the decrease of Y_{BeO} with temperature/c_{D} is due to a decrease of the amount of O-D bonds on the surface as these bonds decrease the binding energy of the O atom to the rest of the material. Above 30 eV, the variation of Y_{BeO} with temperature is mainly due to the evolution of the sputtering of $\mathrm{Be}_x\mathrm{O}_y\mathrm{D}_z$ molecules due to the change in surface damage: as c_{D} decreases, the amount of surface damage decreases as well as Y_{BeO}.

Acknowledgments

The work was perfomed under EUROfusion WP PFC. This work has been carried out within the framework of the EUROfusion Consortium and has received funding from the Euratom research and training programme 2014-2018 and 2019-2020 under grant agreement No

633053. The views and opinions expressed herein do not necessarily reflect those of the European Commission. Grants of computer capacity from CSC-IT Center for Science and the Finnish Grid and Cloud Infrastructure (persistent identifier urn:nbn:fi:research-infras-2016072533) are gratefully acknowledged.

References

[1] V. Philipps, Ph. Mertens, G.F. Matthews, and H. Maier. Overview of the jet iter-like wall project. *Fusion Engineering and Design*, 85(7):1581 – 1586, 2010. Proceedings of the Ninth International Symposium on Fusion Nuclear Technology.

[2] S. Brezinsek. Plasma-surface interaction in the be/w environment: Conclusions drawn from the jet-ilw for iter. *Journal of Nuclear Materials*, 463:11 – 21, 2015. PLASMA-SURFACE INTERACTIONS 21.

[3] A. Loarte, B. Lipschultz, A.S. Kukushkin, G.F. Matthews, P.C. Stangeby, N. Asakura, G.F. Counsell, G. Federici, A. Kallenbach, K. Krieger, A. Mahdavi, V. Philipps, D. Reiter, J. Roth, J. Strachan, D. Whyte, R. Doerner, T. Eich, W. Fundamenski, A. Herrmann, M. Fenstermacher, P. Ghendrih, M. Groth, A. Kirschner, S. Konoshima, B. LaBombard, P. Lang, A.W. Leonard, P. Monier-Garbet, R. Neu, H. Pacher, B. Pegourie, R.A. Pitts, S. Takamura, J. Terry, E. Tsitrone, the ITPA Scrape-off Layer, and Divertor Physics Topical Group. Chapter 4: Power and particle control. *Nuclear Fusion*, 47(6):S203, 2007.

[4] S. Brezinsek, T. Loarer, V. Philipps, H.G. Esser, S. Grünhagen, R. Smith, R. Felton, J. Banks, P. Belo, A. Boboc, J. Bucalossi, M. Clever, J.W. Coenen, I. Coffey, S. Devaux, D. Douai, M. Freisinger, D. Frigione, M. Groth, A. Huber, J. Hobirk, S. Jachmich, S. Knipe, K. Krieger, U. Kruezi, S. Marsen, G.F. Matthews, A.G. Meigs, F. Nave, I. Nunes, R. Neu, J. Roth, M.F. Stamp, S. Vartanian, U. Samm, and JET EFDA contributors. Fuel retention studies with the iter-like wall in jet. *Nuclear Fusion*, 53(8):083023, 2013.

[5] K. Heinola, A. Widdowson, J. Likonen, E. Alves, A. Baron-Wiechec, N. Barradas, S. Brezinsek, N. Catarino, P. Coad, S. Koivuranta, G.F. Matthews, M. Mayer, and P. Petersson. Fuel retention in jet iter-like wall from post-mortem analysis. *Journal of Nuclear Materials*, 463:961 – 965, 2015. PLASMA-SURFACE INTERACTIONS 21.

[6] M. Kumar, C. Makepeace, C. Pardanaud, Y. Ferro, E. Hodille, C. Martin, P. Roubin, A. Widdowson, T. Dittmar, C.h. Linsmeier, C.P. Lungu, C. Porosnicu, I. Jepu, P. Dinca, M. Lungu, O.G. Pompilian, and JET contributors. Identification of beo and beoxdy in melted zones of the jet be limiter tiles: Raman study using comparison with laboratory samples. *Nuclear Materials and Energy*, 17:295 – 301, 2018.

[7] Makepeace C., Pardanaud C., Roubin P., Borodkina I., Ayres C., Coad P., Baron-Wiechec A., Jepu I., Heinola K., Widdowson A., Lozano-Perez S., and J.E.T. Contributors . The effect of beryllium oxide on retention in JET ITER-like wall tiles. *Nuclear Materials and Energy*, 19:346351, 2019.

[8] E A Hodille, J Byggmästar, E Safi, and K Nordlund. Molecular dynamics simulation of beryllium oxide irradiated by deuterium ions: sputtering and reflection. *Journal of Physics: Condensed Matter*, 31(18):185001, mar 2019.

[9] K. Nordlund, M. Ghaly, R. S. Averback, M. Caturla, T. Diaz de la Rubia, and J. Tarus. Defect production in collision cascades in elemental semiconductors and fcc metals. *Phys. Rev. B*, 57:7556–7570, Apr 1998.

[10] J. Tersoff. New empirical model for the structural properties of silicon. *Phys. Rev. Lett.*, 56:632–635, Feb 1986.

[11] J. Tersoff. New empirical approach for the structure and energy of covalent systems. *Phys. Rev. B*, 37:6991–7000, Apr 1988.

[12] C. Björkas, N. Juslin, H. Timko, K. Vörtler, K. Nordlund, K. Henriksson, and P. Erhart. Interatomic potentials for the Be-C-H system. *Journal of Physics: Condensed Matter*, 21(44):445002, 2009.

[13] Donald W. Brenner. Empirical potential for hydrocarbons for use in simulating the chemical vapor deposition of diamond films. *Phys. Rev. B*, 42:9458–9471, Nov 1990.

[14] Paul Erhart, Niklas Juslin, Oliver Goy, Kai Nordlund, Ralf Müller, and Karsten Albe. Analytic bond-order potential for atomistic simulations of zinc oxide. *Journal of Physics: Condensed Matter*, 18(29):6585, July 2006.

[15] J Byggmästar, E A Hodille, Y Ferro, and K Nordlund. Analytical bond order potential for simulations of BeO 1D and 2D nanostructures and plasma-surface interactions. *Journal of Physics: Condensed Matter*, 30(13):135001, 2018.

[16] J. Roth, R. Doerner, M. Baldwin, T. Dittmar, H. Xu, K. Sugiyama, M. Reinelt, Ch. Linsmeier, and M. Oberkofler. Oxidation of beryllium and exposure of beryllium oxide to deuterium plasmas in PISCES B. *Journal of Nuclear Materials*, 438:S1044S1047, 2013. Proceedings of the 20th International Conference on Plasma-Surface Interactions in Controlled Fusion Devices.

[17] J. Roth, W.R. Wampler, M. Oberkofler, S. van Deusen, and S. Elgeti. Deuterium retention and out-gassing from beryllium oxide on beryllium. *Journal of Nuclear Materials*, 453(1):27 – 30, 2014.

[18] V. Kh. Alimov and A. P. Zakharov. *Deuterium Retention In Beryllium and Beryllium Oxide*, pages 247–264. Springer Netherlands, Dordrecht, 2000.

[19] Alexander Stukowski. Visualization and analysis of atomistic simulation data with ovitothe open visualization tool. *Modelling and Simulation in Materials Science and Engineering*, 18(1):015012, 2010.

[20] Etienne A Hodille, Yves Ferro, Zachary Piazza, and Cédric Pardanaud. Hydrogen in beryllium oxide investigated by DFT: on the relative stability of charged-state atomic versus molecular hydrogen. *Journal of Physics: Condensed Matter*, 2018.

[21] J. D. Fowler, Chandra Dipankar, T. S. Elleman, A. W. Payne, and Kuruvilla Verghese. Tritium Diffusion in A12O3 and BeO. *Journal of the American Ceramic Society*, 60(34):155161, 1977.

[22] Y. Hirooka, J. Won, R. Boivin, D. Sze, and V. Neumoin. Effect of impurities on the erosion behavior of beryllium under steady-state deuterium plasma bombardment. *Journal of Nuclear Materials*, 228(1):148153, 1996.

[23] J. Roth, J. Bohdansky, R.S. Blewer, W. Ottenberger, and J. Borders. Sputtering of Be and BeO by light ions. *Journal of Nuclear Materials*, 85-86:10771079, 1979.

[24] J. Roth, W. Eckstein, and J. Bohdansky. Beryllium self-sputtering: An interpolation of data for D, He, Ne and Ar. *Journal of Nuclear Materials*, 165(3):199204, 1989.

[25] M Balden and J Roth. Comparison of the chemical erosion of si, c and sic under deuterium ion bombardment. *Journal of Nuclear Materials*, 279(2):351 – 355, 2000.

[26] M. Schlüter, C. Hopf, T. Schwarz-Selinger, and W. Jacob. Temperature dependence of the chemical sputtering of amorphous hydrogenated carbon films by hydrogen. *Journal of Nuclear Materials*, 376(1):33 – 37, 2008.

[27] E. Salonen, K. Nordlund, J. Keinonen, and C. H. Wu. Swift

chemical sputtering of amorphous hydrogenated carbon. *Phys. Rev. B*, 63:195415, Apr 2001.

[28] D. Nishijima, R.P. Doerner, M.J. Baldwin, and G. De Temmerman. Erosion yields of deposited beryllium layers. *Journal of Nuclear Materials*, 390-391:132 – 135, 2009. Proceedings of the 18th International Conference on Plasma-Surface Interactions in Controlled Fusion Device.

[29] S. Brezinsek, M.F. Stamp, D. Nishijima, D. Borodin, S. Devaux, K. Krieger, S. Marsen, M. O'Mullane, C. Björkas, A. Kirschner, and JET EFDA contributors. Study of physical and chemical assisted physical sputtering of beryllium in the jet iter-like wall. *Nuclear Fusion*, 54(10):103001, 2014.

[30] S. Brezinsek, A. Widdowson, M. Mayer, V. Philipps, P. Baron-Wiechec, J.W. Coenen, K. Heinola, A. Huber, J. Likonen, P. Petersson, M. Rubel, M.F. Stamp, D. Borodin, J.P. Coad, A.G. Carrasco, A. Kirschner, S. Krat, K. Krieger, B. Lipschultz, Ch. Linsmeier, G.F. Matthews, and K. Schmid and. Beryllium migration in JET ITER-like wall plasmas. *Nuclear Fusion*, 55(6):063021, may 2015.

[31] E Safi, G Valles, A Lasa, and K Nordlund. Multi-scale modelling to relate beryllium surface temperature, deuterium concentration and erosion in fusion reactor environment. *Journal of Physics D: Applied Physics*, 50(20):204003, 2017.

[32] C Björkas, D Borodin, A Kirschner, R K Janev, D Nishijima, R Doerner, and K Nordlund. Molecules can be sputtered also from pure metals: sputtering of beryllium hydride by fusion plasmawall interactions. *Plasma Physics and Controlled Fusion*, 55(7):074004, 2013.

[33] Kan Ashida, Masao Matsuyama, Kuniaki Watanabe, Hiroshi Kawamura, and Etsuo Ishitsuka. Secondary ion emission from beryllium surfaces by ar and /or (ar+d2) mixed ion bombardments. *Journal of Nuclear Materials*, 210(3):233 – 238, 1994.

[34] S. Brezinsek, A. Pospieszczyk, G. Sergienko, R. Dux, M. Cavedon, M. Faitsch, and K. Krieger. Chemically assisted physical sputtering of tungsten: Identification via the 66+ transition of wd in textor and asdex upgrade plasmas. *Nuclear Materials and Energy*, 18:50 – 55, 2019.

[35] Linn W. Hobbs. Topology and geometry in the irradiation-induced amorphization of insulators. *Nuclear Instruments and Methods in Physics Research Section B: Beam Interactions with Materials and Atoms*, 91(1):30 – 42, 1994.

[36] A. Allouche and Y. Ferro. First-Principles Study of hydrogen retention and diffusion in beryllium oxide. *Solid State Ionics*, 272:91100, 2015.

View publication stats